
CASE REPORT

Two-staged reconstruction for ankylosed hip with severe limb shortening: a case report

Koji Goto¹, Kazutaka So¹, Yutaka Kuroda¹, Keiichi Kawanabe², Shuichi Matsuda¹

¹ Department of Orthopaedic Surgery, Kyoto University, Kyoto - Japan

² Department of Orthopaedic Surgery, Shiga Medical Centre for Adults, Shiga - Japan

A 58-year-old man developed a 14 cm limb length discrepancy with a shortened and ankylosed right hip as a sequelae of multiple surgeries for recurrent dislocation and periprosthetic joint infection. He was successfully treated by limb elongation with external fixation and subsequent revision total hip arthroplasty. We discuss the efficacy of the two-staged reconstruction with initial limb elongation.

Keywords: Ankylosis, Limb elongation, External fixation, Revision total hip arthroplasty

Accepted: October 7, 2014

INTRODUCTION

Multiple hip surgeries to address the complications of total hip arthroplasty (THA) can cause severe bone defects, limb shortening, and disability (1). We present a patient with hip joint ankylosis and massive bone loss in the presence of a cement spacer surrounded by ectopic bone formation secondary to the sequelae of multiple revision hip surgery for recurrent dislocation and PJI. The two-staged approach with limb elongation using external fixation equipment was adopted initially and subsequent revision with a megaprosthesis (2).

CASE REPORT

A 58-year-old man was injured in a traffic accident and treated for traumatic posterior dislocation of his right hip with concomitant acetabular rim fracture. Afterwards, THA was performed for recurrent dislocation. The THA subsequently dislocated and the acetabular component was revised to a constrained-type socket. This was then complicated by postoperative prosthetic joint infection (PJI) with methicillin-resistant *Staphylococcus aureus* (MRSA). An articulating cement spacer with antibiotics was performed

but failed to control the PJI. The infected circumferential bony structures were excised and a bulky antibiotic-impregnated cement spacer was left in the joint for infection control. While the infection subsided, limb shortening progressed and ectopic ossification occurred around the joint, which resulted in ankylosis of the hip. He could no longer ambulate without crutches and was referred to our clinic 1 year later.

On initial physical examination at our hospital, the right hip was ankylosed in 10° flexion, 5° abduction, and 70° external rotation and there was a leg-length discrepancy of 14 cm. The Merle d'Aubigne-Postel score was 2 points.

Physical findings and blood analysis indicated no signs of infection. Radiographic examination, including computed tomography, showed that the hip joint was occupied by the cement spacer surrounded by large amounts of ectopic ossification. A large bony defect of the acetabulum and proximal femur was also found (Fig. 1).

To correct the leg length discrepancy of 14 cm, a two-stage reconstruction strategy was planned. In the first surgery, the external fixation device was applied to elongate the right limb as much as possible. In addition, meticulous debridement was carried out to remove the cement spacer and ectopic ossification. Both the tissue culture and

histological examination indicated no PJI. The proximal fixation pins were screwed into the iliac wing, and the distal fixation pins were screwed into the femoral shaft using the Ace-Fisher external fixation system (DePuy ACE, Warsaw, Indiana, USA). Following this, the semi-circular frames and 3 connection rods were fixed firmly. Then antibiotic-impregnated cement beads (1-2 cm in diameter) were left in the joint space to secure prosthesis accommodation and prevent re-infection (Fig. 2a).

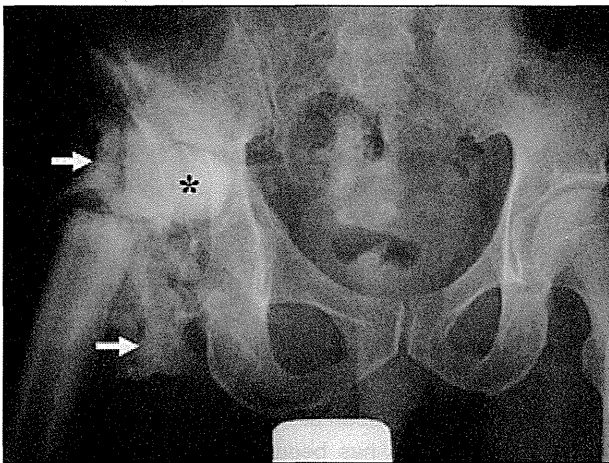


Fig. 1 - An AP radiograph of the hip joint. The proximal femur was resected, and the proximal stump was at the isthmus. White arrows represent ectopic ossifications. Asterisk represents cement spacer.

To avoid excessive stress to the proximal fixation pins, which were not inherently rigid, 1-2 mm elongation each day was performed. The ipsilateral nerve and blood vessels were observed closely to detect any possible damage to them due to over-extension. Neither neuro-vascular complications nor complications associated with the external fixation device were encountered during the lengthening process. Finally, elongation of 10 cm was obtained successfully 2 months later (Fig. 2b)

The removal of the external fixator and revision THA were then performed in 1 operative session 2 months after our initial surgery. For acetabular reconstruction, bulk and impaction allograft bone grafting was performed with acetabular augmentation with a KT plate (KYOCERA Medical Corporation, Osaka, Japan). This plate is used in Japan as an anti-protrusion device like the Müller ring (3). Then a highly cross-linked, ultra-high-molecular-weight polyethylene liner (Excell-link: KYOCERA) and limb salvage femoral megaprosthesis (PHS type-1 long stem: KYOCERA) were fixed with antibiotic laden cement, and a 28 mm Zirconia head (KYOCERA) was applied. Gait exercise started with half weight-bearing at 2 weeks postoperatively, and full weight-bearing started at 12 weeks postoperatively.

At the latest follow-up, 7 years after revision, examination showed that the patient had mild thigh pain presumably due to residual heterotopic ossification, and required a shoerise for his right foot. He could walk without a cane although with

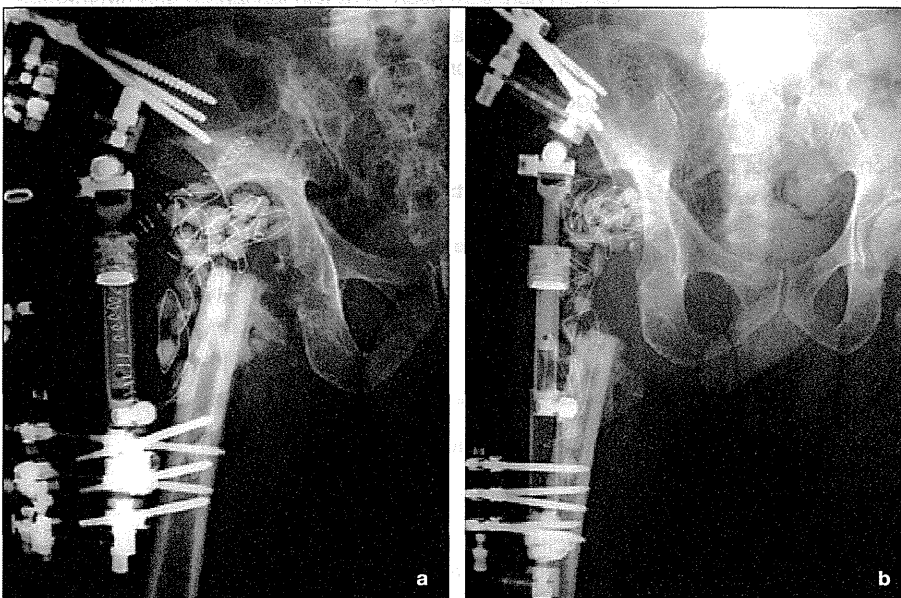


Fig. 2 - AP radiograph: a) just after the initial surgery; b) at 2 months after the initial surgery.



Fig. 3 - AP radiograph after revision THA at 7 years postoperatively.

a slight limp. The final Merle d'Aubigne-Postel score was 16 points with 6 points for pain, 5 points for walking ability, and 5 points for mobility. Radiological examination demonstrated no signs of loosening (Fig. 3).

DISCUSSION

Recent reports on PJI and dislocation after total hip arthroplasty reveal a decreased rate of occurrence of both PJI (4, 5) and dislocation (6). However, if PJI has occurred previously, it may require multiple joint surgeries, leading to massive bone loss and severe dysfunction of the limb. This rare case with excessive shortening of the lower limb and joint ankylosis represents the possible complications of multiple joint surgeries. In this case, because of the 14 cm limb length discrepancy, it was impossible to obtain both satisfactory joint function and walking ability with revision THA before adequate limb elongation was achieved.

The external fixation technique has many merits (7-9). In particular, it can regulate the elongation of the limb without

any material-induced damage to the focal joint. Though it would be desirable for the half pins to be inserted far from the joint space to avoid recurrence of PJI secondary to pin tract infection, we could not elongate the distance between the joint space and the distal half pins more because of the length limitation of the external fixation device. There was eventually no pin-tract infection.

In this case, there was a potential risk of joint instability at the second surgery because of the massive bone defect and muscular impairment. However, we did not use constrained acetabular components because the patient was under the age of 60 and there was a concern for the long-term clinical results of revision THA with their use (10, 11).

Some of the possible disadvantages of this two-stage method include longer bed rest with limited motion that may cause deep venous thrombosis and decubitus ulcer during the period of limb elongation and the potential risk of pin tract infection. However, these potential disadvantages can be overcome and the substantial negative influences on the patient can be minimised with attentive nursing care.

Although similar application of the external fixator in treating hip joint diseases has been reported in few studies (12-14), successful elongation of over 10 cm at the hip joint combined with two-stage revision hip arthroplasty using a megaprosthesis has not been previously reported in the English literature. While the two-stage method presented here was used to regain leg length and hip function successfully, cases with intractable periprosthetic instability or infection should be treated properly at an earlier stage.

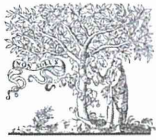
Financial Support: None.

Conflict of Interest: None.

Address for correspondence:
Koji Goto
Department of Orthopaedic Surgery
Kyoto University
54 Shogoin-kawahara-cho
Sakyo-ku
Kyoto City
Kyoto 606-8507, Japan
k.g.bau@kuhp.kyoto-u.ac.jp

REFERENCES

1. Parvizi J, Sim FH. Proximal femoral replacements with mega-prostheses. *Clin Orthop Relat Res.* 2004;(420):169-175.
2. Lundh F, Sayed-Noor AS, Brosjö O, Bauer H. Megaprosthetic reconstruction for periprosthetic or highly comminuted fractures of the hip and knee. *Eur J Orthop Surg Traumatol.* 2014; 24(4):553-557.
3. Berry DJ, Müller ME. Revision arthroplasty using an anti-protrusion cage for massive acetabular bone deficiency. *J Bone Joint Surg Br.* 1992;74(5):711-715.
4. Pulido L, Ghanem E, Joshi A, Purtill JJ, Parvizi J. Periprosthetic joint infection: the incidence, timing, and predisposing factors. *Clin Orthop Relat Res.* 2008;466(7):1710-1715.
5. Phillips JE, Crane TP, Noy M, Elliott TS, Grimer RJ. The incidence of deep prosthetic infections in a specialist orthopaedic hospital: a 15-year prospective survey. *J Bone Joint Surg Br.* 2006;88(7):943-948.
6. Caton JH, Prudhon JL, Ferreira A, Aslanian T, Verdier R. A comparative and retrospective study of three hundred and twenty primary Charnley type hip replacements with a minimum follow up of ten years to assess whether a dual mobility cup has a decreased dislocation risk. *Int Orthop.* 2014;38(6):1125-1129.
7. Rose RE, Wright DE. Treatment of congenital pseudarthrosis of the tibia with the Ilizarov technique. Case report and review of the literature. *West Indian Med J.* 2007;56(3):294-299.
8. Hosalkar HS, Jones S, Chowdhury M, Hartley J, Hill RA. Quadricepsplasty for knee stiffness after femoral lengthening in congenital short femur. *J Bone Joint Surg Br.* 2003;85(2):261-264.
9. Liu T, Zhang X, Li Z, Zeng W. Reconstruction with tibial lengthening for limb length discrepancy in Crowe Type IV developmental dysplasia of hip in adulthood. *Eur J Orthop Surg Traumatol.* 2013;23(2):225-231.
10. Pattyn C, De Haan R, Kloeck A, Van Maele G, De Smet K. Complications encountered with the use of constrained acetabular prostheses in total hip arthroplasty. *J Arthroplasty.* 2010;25(2):287-294.
11. Khan RJ, Fick D, Alakeson R, Li MG, Nivbrant B, Wood D. The constrained acetabular component for hip instability. *J Arthroplasty.* 2007;22(3):377-382.
12. Onoda S, Hatori M, Yamada N, Hosaka M, Kokubun S. A two-stage surgery for severe femoral neck deformity due to fibrous dysplasia: a case report. *Ups J Med Sci.* 2004;109(2):123-129.
13. Lai KA, Shen WJ, Huang LW, Chen MY. Cementless total hip arthroplasty and limb-length equalization in patients with unilateral Crowe type-IV hip dislocation. *J Bone Joint Surg Am.* 2005;87(2):339-345.
14. Brinker MR, Mathews V, O'Connor DP. Ilizarov distraction before revision hip arthroplasty after resection arthroplasty with profound limb shortening. *J Arthroplasty.* 2009;24(5):826.e17-23.



ELSEVIER

Contents lists available at ScienceDirect

The Veterinary Journal

journal homepage: www.elsevier.com/locate/tvj

Multipotency of equine mesenchymal stem cells derived from synovial fluid

D. Murata^a, D. Miyakoshi^b, T. Hatazoe^c, N. Miura^a, S. Tokunaga^a, M. Fujiki^a,
K. Nakayama^d, K. Misumi^{a,*}

^a Faculty of Veterinary Medicine, Kagoshima University, 21-24 Korimoto 1-chome, Kagoshima 890-0065, Japan

^b Hidaka Horse Breeders Association, 175-2 Shizunai-Shinmori, Shinhidaka-cyo, Hidaka-gun, Hokkaido 056-0002, Japan

^c Kyushu Stallion Station, The Japan Bloodhorse Breeders' Association, 3995 Nagata, Osaki-cho, Soo-gun, Kagoshima 899-8313, Japan

^d Graduate School of Science and Engineering, Saga University, 1 Honjyo-cho, Saga 840-8502, Japan

ARTICLE INFO

Article history:

Accepted 31 July 2014

Keywords:

Equine
Synovial fluid
Mesenchymal stem cells
Differentiation

ABSTRACT

Cartilage regeneration with cell therapy following arthroscopic surgery could be used in racehorses with intra-articular fractures (IAF) and osteochondritis dissecans (OCD). The aims of this study were to investigate the origin and multipotency of stromal cells in the synovial fluid (SF) of horses with intra-articular injury and synovitis, and to provide a new strategy for regeneration of lost articular cartilage. Mesenchymal stromal cells were isolated from SF of horses with IAF and OCD. Multipotency was analysed by RT-PCR for specific mRNAs and staining for production of specific extracellular matrices after induction of differentiation. The total number of SF-derived mesenchymal stromal cells reached $>1 \times 10^7$ by the fourth passage. SF-derived cells were strongly positive (>90% cells positive) for CD44, CD90 and major histocompatibility complex (MHC) class I, and moderately positive (60–80% cells positive) for CD11a/CD18, CD105 and MHC class II by flow cytometry. SF-derived cells were negative for CD34 and CD45. Under specific nutrient conditions, SF-derived cells differentiated into osteogenic, chondrogenic, adipogenic and tenogenic lineages, as indicated by the expression of specific marker genes and by the production of specific extracellular matrices. Chondrogenic induction in culture resulted in a change in cell shape to a 'stone-wall' appearance and formation of a gelatinous sheet that was intensely stained with Alcian blue. SF may be a novel source of multipotent mesenchymal stem cells with the ability to regenerate chondrocytes.

© 2014 Elsevier Ltd. All rights reserved.

Introduction

Arthroscopic surgery to remove osteochondral fragments and to curette the surrounding degenerative cartilage has been accepted worldwide in Thoroughbred horses with intra-articular fractures (IAFs) and osteochondritis dissecans (OCD). To repair defects with hyaline cartilage, cartilage regeneration using mesenchymal stem cells (MSCs) derived from bone marrow (BM) (Arnhold et al., 2007) or adipose tissue (AT) (Braun et al., 2010) has been investigated.

The advantage of AT-MSCs is the abundance of MSCs per unit weight of tissue (Burk et al., 2013). However, we believe that a therapeutic strategy using AT-MSCs may be unacceptable in racehorse practice, because of the lower somatic fat quantities in Thoroughbred horses compared to Standardbred horses (Kearns et al., 2001). Paracentesis to aspirate BM is invasive and must be done with care to avoid contamination (Vidal et al., 2007).

Stem cells are increased in the synovial fluid (SF) of human beings with joint disease and injury (Jones et al., 2004; Morito et al., 2008). Improved clinical outcomes have been reported following treatment of cartilage deficits in human beings using MSCs derived from the synovium and SF (Nimura et al., 2008; Lee et al., 2011; Sekiya et al., 2012; Suzuki et al., 2012). If MSCs can be isolated from SF and expanded over a short time period after a racehorse is injured, they may be useful as a new strategy for cartilage regeneration. The aims of this study were to investigate the proliferative capacity, phenotypic characteristics and multipotency of cells in the SF associated with intra-articular injury and synovitis, and to provide a new strategy for regenerating lost or damaged cartilage with SF-MSCs.

Materials and methods

Samples

SF (3–4 mL per joint) was collected aseptically from the carpal, fetlock or tarsal joints of 11 Thoroughbred horses with IAF or OCD at the time of arthroscopic surgery (Table 1). SF samples were also obtained from nine diseased and nine normal Thoroughbred horse joints to compare the number of MSCs in the SF (Table 2). AT and BM were collected from two other horses (a male aged 10 years and a female aged

* Corresponding author. Tel.: +81 99 2858731.

E-mail address: kaz_msm@vet.kagoshima-u.ac.jp (K. Misumi).

Table 1

Profiles of synovial fluid (SF) samples obtained from the joints of horses with intra-articular fractures (IAFs) or osteochondritis dissecans (OCD).

Sample number	Age (years)	Sex	Disease	Diseased site (limb/joint)	Period of clinical onset (weeks)
1	3	F	IAF	RF/Carpus	2
2	2	F	IAF	RF/Fetlock	4
3	2	F	IAF	LF/Fetlock	4
4	1	F	IAF	LH/Tarsus	3
5	1	F	OCD	LH/Tarsus	3
6	3	M	IAF	RF/Carpus	2
7	3	F	IAF	RF/Carpus	2
8	3	M	IAF	RF/Carpus	2
9	3	M	IAF	RF/Carpus	2
10	6	M	IAF	RH/Tarsus	2
11	1	F	OCD	LH/Tarsus	No signs

SF samples were aseptically obtained from carpal, fetlock or tarsal joints of 11 Thoroughbred horses with IAF or OCD. M, male; F, female; RF, right forelimb; LF, left forelimb; RH, right hind limb; LH, left hind limb.

3 years) that were free of any joint diseases. All procedures were approved by the Animal Care and Use Committee of Kagoshima University (approval number A11037; date of approval 26 March 2012).

Isolation and expansion of stromal cells from synovial fluid

SF was diluted with five volumes of phosphate buffered saline (PBS), filtered through a 70 µm nylon filter (Cell Strainer, BD Falcon) to remove debris and centrifuged at 160 g for 5 min at room temperature. After decanting the supernatant, the pellet was resuspended and plated in a 25 cm² culture flask in complete culture medium (CCM) consisting of Dulbecco's Modified Eagle's Medium (DMEM, Life Technologies), 10% fetal bovine serum (FBS, Thermo Scientific) and 1% antibiotic-antifungal preparation (100 U/mL Penicillin G, 100 µg/mL streptomycin, 0.25 µg/mL amphotericin B; Antibiotic-Antimycotic, Life Technologies). After incubation at 37 °C in 5% CO₂ for 9 days, cells adhering to the bottom of the flask were washed with PBS and harvested as described below. The medium was changed on days 4 and 7 (D7; Passage 0, P0). The number of colonies was counted at P0 in the 18 SF samples from the nine diseased and nine normal horse joints (Table 2).

Cultured cells were harvested with 0.05% trypsin and 0.2 mM ethylene diamine tetraacetic acid (Trypsin-EDTA, Life Technologies), and centrifuged. After decanting the supernatant, the pellet was rinsed with CCM and the cells were replated at 1 × 10⁶ cells in 150 cm² dishes and cultured for 9 days. The medium was changed every 3 days for 9 days (P1). This serial process of passaging was repeated to obtain >1 × 10⁷ cells for reverse transcription (RT)-PCR and flow cytometry. The total number of cells was determined with a cell counter at every passage from P1 to determine proliferation rates, which were calculated as the cell doubling number, cell doubling time and daily duplication rate using the following formulas:

$$\text{Cell doubling number} = \ln(\text{final number of cells}/\text{initial number of cells})/\ln(2)$$

$$\text{Cell doubling time} = \text{Cell culture time}/\text{cell doubling number}$$

$$\text{Daily duplication rate} = \text{Cell doubling number}/\text{cell culture time} \\ = 1/\text{cell doubling time}$$

Surface markers and multipotency of the cells were analysed at the fifth passage (P5). Normal SF-MSCs were analysed at P6, when sufficient numbers of cells were obtained.

Isolation and expansion of stromal cells from adipose tissue and bone marrow

Horses were sedated by IV injection with 4 µg/kg medetomidine HCl (Domitor, Zenoaq) and 10 µg/kg butorphanol tartrate (Vetorphale, Meiji Seika), and 25–30 g AT were obtained from the gluteal subcutis using liposuction. Liposuction solution (100–200 mL) consisting of physiological saline (Normal Saline, Otsuka) containing 400 µg/mL lignocaine HCl and 0.4 µg/mL adrenaline (Xylocaine injection 1% with Epinephrine, AstraZeneca) was injected SC through a 10 mm skin incision and AT was aspirated with a probe (Collection Cannula, 14 G, length 30 cm; Cytori) connected to a 50 mL syringe. This procedure was repeated 10 times. The aspirated AT was digested with a 2× volume of PBS containing 0.1% collagenase (Life Technologies) at 37 °C for 90 min, filtered through a 70 µm nylon filter (Cell Strainer, BD Falcon) and centrifuged at 160 g for 5 min at room temperature. The cell pellet was re-suspended in CCM and incubated at 37 °C in 5% CO₂ for 9 days, then cells adhering to the bottom of the flask were washed with PBS and harvested. The medium was changed on the day 6 (D6; P0).

BM (30–35 mL) was collected from the fifth segment of the sternum by needle core biopsy under local anaesthesia with 20 mg/mL lignocaine HCl (Xylocaine Injection 2%, AstraZeneca) and the same sedatives and analgesics as used for AT collection. A bone marrow biopsy needle (11 G, length 10.2 cm; Angiotech) was inserted through a 10 mm skin incision. BM was aspirated with a 20 mL syringe containing 5000 IU heparin, then re-suspended in CCM. After incubation at 37 °C in 5% CO₂ for 9 days, the cells adhering to the bottom of the flask were washed with

Table 2

Colonies of normal and diseased equine synovial fluid (SF)-derived mesenchymal stem cells at passage 0.

Source of stem cells	Sample number	Disease	Limb/Joint	Colonies at passage 0	Mean ± standard deviation	P value
SF from diseased joints	D1	IAF	RF/Carpus	73	166.9 ± 100.9	0.001
	D2	IAF	RF/Carpus	62		
	D3	IAF	LF/Carpus	94		
	D4	IAF	RF/Carpus	121		
	D5	IAF	LF/Carpus	364		
	D6	IAF	RF/Carpus	271		
	D7	OCD	RH/Tarsus	161		
	D8	IAF	RF/Carpus	136		
	D9	IAF	RF/Carpus	220		
SF from normal joints	N1	ND	LF/Carpus	10	8.3 ± 6.5	
	N2	ND	LF/Carpus	21		
	N3	ND	LF/Carpus	10		
	N4	ND	RF/Carpus	5		
	N5	ND	LF/Carpus	6		
	N6	ND	LH/Tarsus	3		
	N7	ND	RF/Carpus	5		
	N8	ND	RH/Tarsus	0		
	N9	ND	LF/Carpus	13		

SD, standard deviation; IAF, intra-articular fractures; OCD, osteochondritis dissecans; ND, no data; RF, right forelimb; LF, left forelimb; RH, right hind limb; LH, left hind limb.

Table 3

Reverse transcriptase PCR primer sequences, annealing temperatures and amplification product sizes for multipotent, osteogenic, chondrogenic, adipogenic and tenogenic genes.

Marker	Gene	Sequence (Forward/Reverse)	Annealing temperature (°C)	Fragment (base pairs)
Multipotency	Nanog	5'-TACCTCAGCCTCCAGCAGAT-3' 5'-CATTGGTTTTCTGCCACT-3'	58.0	190
	Sox2	5'-TGGTTACCTCTCTCCACT-3' 5'-GGGCAGTGTGCCGTTAAT-3'	58.0	179
Osteogenesis	Runx2	5'-TGTCAATGCGGGTAACGAT-3' 5'-TCCGGCCCAAACTCTCA-3'	61.3	107
	ALP	5'-GCTGGGAAATCCGTGGCATTGTG-3' 5'-CGGCAGAGTGGCGTAGG-3'	64.3	81
	OC	5'-GAGGGCAGTGGTGGTGAAG-3' 5'-CTCTGGAAGCCGATGTGGTC-3'	63.3	152
Chondrogenesis	Sox9	5'-AGTACCCGACCTGCACAAC-3' 5'-CGCTTCTCGCTCTCGTTTCA-3'	50.0	79
	Col-2	5'-GCTTCCACTTCAGCTATGGA-3' 5'-TGTTTCGTGCAGCCATCCTT-3'	56.9	256
	AGG	5'-TGCACAGACCCGCCAGCTA-3' 5'-GTCTTAAACTCAGTCCAGC-3'	51.4	339
Adipogenesis	PPAR γ 2	5'-GTCTATAACGCCATCAGTTTG-3' 5'-GCCCTCGCTTCGCTTTG-3'	50.0	180
Tenogenesis	Scx	5'-TCTGCCTCAGCAACAGAGA-3' 5'-TCCGAATCGCCGTCTTTC-3'	58.0	59
	TenC	5'-GATCTTCACTTCCCTACCAACG-3' 5'-CTCATCCAGCATGGGGTC-3'	58.0	70
Housekeeping	GAPDH	5'-ACCACAGTCCATGCATCAC-3' 5'-TCCACCACCCTGTTGCTGTA-3'	60.0	450

Nanog, homeobox protein NANOG; Sox2, sex determining region Y-box 2; GAPDH, glyceraldehyde-3-phosphate dehydrogenase; ALP, alkaline phosphatase; OC, osteocalcin; Sox9, sex determining region Y-box 9; Col-II, type II collagen; AGG, aggrecan; PPAR γ 2, peroxisome proliferator activated receptor γ 2; Scx, scleraxis; TenC, tenascin C.

PBS and harvested as described above. The medium was changed on the day 6 (D6; P0).

Expression of multipotency markers by stromal cells from synovial fluid

Total RNA from cultured cells was isolated using the mirVana miRNA Isolation Kit (Life Technologies) and converted to cDNA by RT using the TaKaRa RT-PCR system (PCR Thermal Cycler MP, TaKaRa) and RT-PCR kit (ReverTra Dash, Toyobo), with a 20 min incubation at 42 °C, followed by a 5 min incubation at 99 °C to inactivate the RT. PCR primers and expected sizes of products for homeobox protein Nanog and sex determining region Y-box 2 (Sox2) are summarised in Table 2. PCR conditions were 30 cycles of 98 °C for 10 s, individual annealing temperature for 2 s (Table 3) and 74 °C for 15 s. The reaction products were separated by electrophoresis on 1.5% agarose gels and the expression of multipotency markers was determined based on the expected size of the bands labelled with SYBR green.

Flow cytometry

Cells (1×10^4) were resuspended in 500 μ L staining buffer (SB; PBS containing 1% FBS) and incubated for 30 min at 4 °C with 20 μ g/mL antibodies that recognise CD11a/CD18, CD34, CD44, CD45, CD90, CD105 and major histocompatibility complex (MHC) classes I and II (Table 4). Prior to incubation with cells, antibodies against CD11a/CD18, CD44 and MHC classes I and II were coupled with secondary antibodies conjugated to fluorescein isothiocyanate (FITC). Non-specific FITC mouse immunoglobulin G1 κ was used as a negative control. FITC-labelled cells were washed with SB and resuspended in 500 μ L SB for fluorescence-activated cell sorting (FACS). Cell fluorescence was evaluated as a strong shift in the mean fluorescence

intensity (MFI) by flow cytometry using a FACS Aria II instrument. The data were analysed using FACS Diva software.

Induction and evaluation of differentiation

To investigate osteogenic differentiation, cells were plated in 6-well plates (6 Well Plate-N, Nest Biotech) in CCM at an initial density of 2.5×10^3 cells/cm². After 24 h incubation, CCM was replaced with osteogenic induction medium (Differentiation Basal Medium-Osteogenic, Lonza) supplemented with 100 μ M ascorbic acid, 10 mM β -glycerophosphate and 1 μ M dexamethasone. After 2 weeks in induction medium, total RNA from the plate-cultured cells was prepared as described above and expression of the osteoblast-specific genes runt-related transcription factor 2 (Runx2), alkaline phosphatase (ALP) and osteocalcin (OC) were analysed. PCR primers, amplification conditions and the expected sizes of the products are summarised in Table 3. Negative controls for RT-PCR products were obtained from SF-derived stromal cells that were not placed in induction medium (data not shown).

Chondrogenic differentiation was induced in aggregate and plate cultures for 2 weeks. Cells (5×10^5) were resuspended in a 15 mL centrifuge culture tube (SuperClear Centrifuge Tubes, Labcon) in 500 μ L chondrogenic induction medium (Differentiation Basal Medium-Chondrogenic, Lonza) supplemented with 4.5 g/L D-glucose, 350 μ M L-proline, 100 nM dexamethasone and 0.02 g/L transforming growth factor (TGF)- β 3. Another aliquot of 5×10^4 cells was resuspended in a 6-well plate in 2 mL induction medium, which was replaced three times per week, similar to osteogenic induction. Two weeks later, total RNA from the plate-cultured cells was prepared as described above and expression of chondrogenic marker genes, including sex determining region Y-box 9 (Sox9), type II collagen (Col-II) and aggrecan, was examined (Table 3). Production of mucopolysaccharide in the chondrogenic extracellular matrix

Table 4

Antibodies for analysing the specific molecular markers on the cell surface.

Antibody	Company	Clone	Epitope	Dilution
CD11a/CD18	Gift ^a	CZ3.2, 117, 2E11, B10	Not confirmed	1:10
CD34	BD Bioscience	581/CD34	O-glycosylated transmembrane glycoprotein	1:5
CD44	AbD Serotec	CVS18	Not confirmed	1:10
CD45	BD Bioscience	2D1	T200 family	1:2.5
CD90	BD Bioscience	5E10	Not confirmed	1:10
CD105	AbD Serotec	SN6	Glycoprotein homodimer	1:10
MHC class I	Gift ^a	CZ3, 117, 1B12, C11	Not confirmed	1:10
MHC class II	Gift ^a	CZ11, 130, 8E8, D9	Not confirmed	1:10
Secondary (FITC)	Rockland	-	Mouse IgG (H and L)	1:500
Isotype control	BD Bioscience	MOPC-21	Not confirmed	1:10

^a The antibodies against CD11a/18 and MHC classes I and II were gifts from Dr Douglas Antczak, Cornell University, Ithaca, New York, USA. MHC, major histocompatibility complex; FITC, fluorescein isothiocyanate.

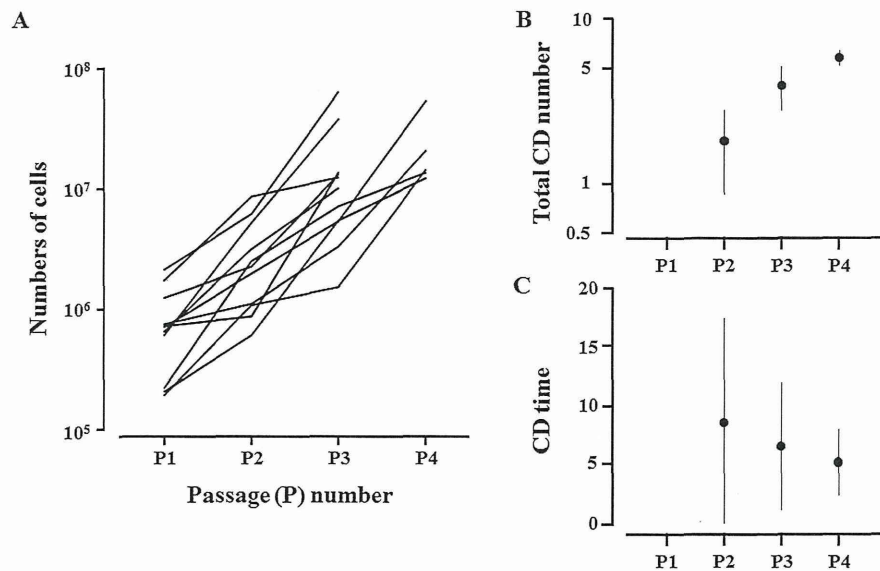


Fig. 1. Growth curves (a), total cell doubling numbers (b) and cell doubling (CD) times (c) from passages 0 to 4 (P0–P4) of synovial fluid (SF)-derived mesenchymal stem cells (MSCs) collected from 11 horses. Six samples produced $>1 \times 10^7$ cells at P3 and five samples required ~6 weeks to reach $>1 \times 10^7$ cells (at P4). CD number = $\ln(N_f / N_i) / \ln(2)$. CD time = cell culture time / CD number. N_f , final number of cells; N_i , initial number of cells.

was determined by staining with Alcian blue in 6-well plates. The differentiated cells were fixed onto the culture plate by methanol, then treated with 3% acetic acid. The plates onto which the cells adhered were stained with Alcian blue (pH 2.5) for 90 min.

Cell aggregates were fixed with 10% neutral buffered formalin, dehydrated in graded series of ethanol, embedded in paraffin, sectioned at 5 μ m thickness and mounted on glass slides. After dehydration with methanol and treatment with 3% acetic acid, cell aggregates were stained with Alcian blue (pH 2.5) for 90 min to detect cartilage-specific proteoglycans, then counterstained with Mayer's haematoxylin. The sections were also analysed immunohistochemically with an antibody against car-

tilage oligomeric matrix protein (COMP; catalogue number ab91354, Abcam). Following deparaffinisation and rehydration, the sections were treated with blocking buffer (0.01 M PBS containing 0.25% casein), then incubated with primary antibody (diluted 1:100 in blocking buffer) overnight. The slides were incubated with secondary biotinylated goat anti-rabbit IgG (Polyclonal Goat Anti-Rabbit Immunoglobulins/Biotinylated; catalogue number E0432, DakoCytomation; diluted 1:300), for 30 min. Secondary antibodies were labelled with avidin-biotin-horseradish peroxidase complex (ABC standard kit, VectaStain) and visualised after treatment with 3, 3'-diaminobenzine.

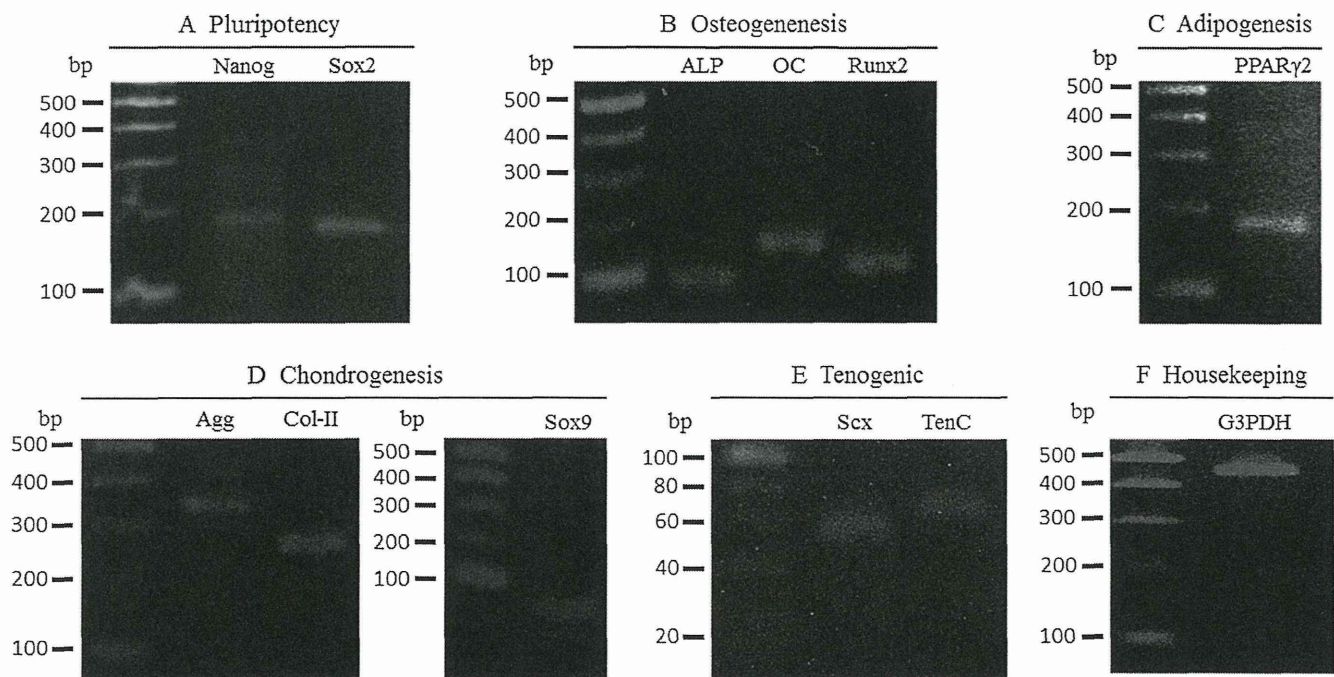


Fig. 2. Results of reverse transcriptase-PCR using specific marker genes of multipotency, and osteogenic, chondrogenic, adipogenic and tenogenic differentiation. Nanog, homeobox protein NANOG; Sox2, sex determining region Y-box 2; Runx2, runt-related transcription factor 2; ALP, alkaline phosphatase; OC, osteocalcin; Sox9, sex determining region Y-box 9; Col2, type II collagen; Agg, aggrecan; PPAR γ 2, peroxisome proliferator activated receptor γ 2; Scx, scleraxis; TenC, tenascin C; G3PDH, glyceraldehyde-3-phosphate dehydrogenase.

Table 5

Percentages (%) of positive cells to specific molecular markers by flow cytometry.

	Diseased SF-MSCs	Normal SF-MSCs	BM-MSCs	AT-MSCs
CD11a/CD18	73.7 ± 2.3	61.6 ± 3.2	80.1 ± 1.1	79.6 ± 5.5
CD34	0.3 ± 0.2	0.3 ± 0.2	0.4 ± 0.1	1.0 ± 0.2
CD44	98.1 ± 0.6	97.9 ± 0.5	96.8 ± 0.0	95.6 ± 2.4
CD45	0.2 ± 0.1	0.2 ± 0.1	0.4 ± 0.1	1.0 ± 0.8
CD90	99.0 ± 0.4	96.0 ± 3.7	98.5 ± 0.7	98.7 ± 0.8
CD105	73.5 ± 6.0	77.9 ± 1.6	50.2 ± 27.2	77.1 ± 14.5
MHC-I	94.6 ± 3.3	95.9 ± 1.6	90.8 ± 6.5	94.5 ± 2.6
MHC-II	71.9 ± 4.1	74.9 ± 3.0	78.1 ± 3.9	79.3 ± 7.7

SF, synovial fluid; BM, Bone marrow; AT, adipose tissue; MSCs, mesenchymal stem cells; MHC, major histocompatibility complex.

Adipogenic differentiation was induced when cells reached a density of 15,000 cells/cm² on 6-well plates in basal medium. After pre-incubation for 24 h, CCM was replaced with adipogenic induction medium, composed of DMEM supplemented with 4.5 g/L *D*-glucose, 100 μM indomethacin, 10 μg/mL insulin, 0.5 mM 3-isobutyl-1-methylxanthine, 1 μM dexamethasone and 5% rabbit serum. Seven days later, total RNA from the cells was isolated as described above and evaluated for expression of the adipogenic marker gene peroxisome proliferator activated receptor γ2 (PPARγ2) (Table 3). Adipocyte-specific intracellular lipids were stained with oil red O.

Tenogenic differentiation was induced when cells reached a density of 15,000 cells/cm² on 6-well plates in CCM. After incubation for 24 h, 50 ng/mL bone morphogenetic protein (BMP) 12 (Recombinant Human BMP-12/GDF-7, BioVision) was added to CCM for tenogenic induction. Following 2 weeks in induction medium, total RNA from the plate-cultured cells was prepared as described above, and expression of scleraxis (Scx) and tenascin C (TenC) as tenocyte- and tenogenesis-specific genes were analysed (Table 3).

Statistical analysis

All quantitative group data are shown as the mean ± standard deviation (SD). Data were analysed using Student's *t* test (Excel, Microsoft). Differences of *P* < 0.01 were considered to be statistically significant.

Results

Isolation and expansion of stromal cells

SF-derived MSCs adhering to the bottom of the culture flask were spindle-shaped and present as a minority of the cell components. At P0, the total number of colonies of SF-MSCs from diseased joints

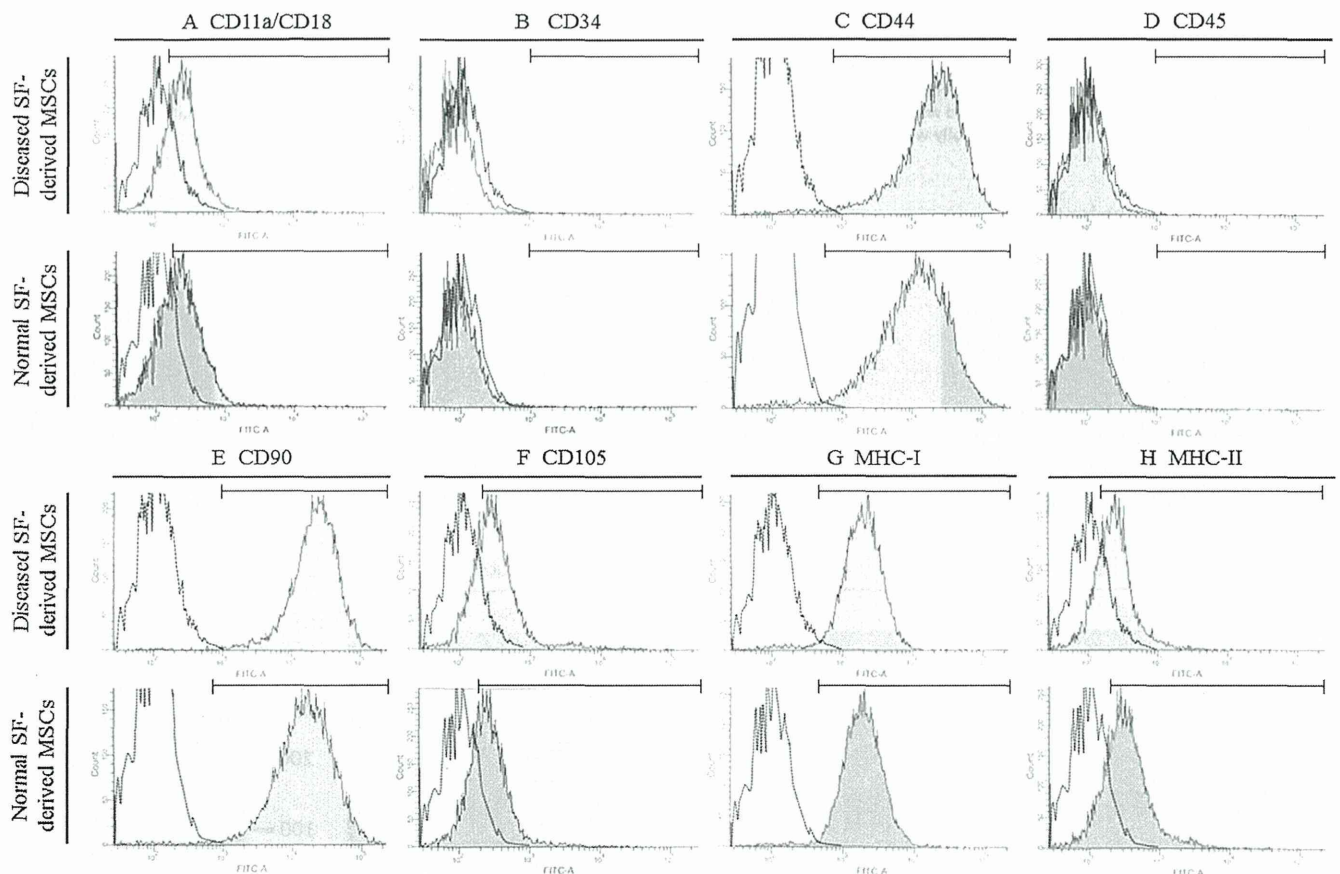


Fig. 3. Results of flow cytometry using immunological markers on synovial fluid (SF)-derived mesenchymal stem cells (MSCs) from normal and diseased joints. A strong shift in mean fluorescence intensity (MFI) was detected with antibodies against CD44 (C), CD90 (E) and major histocompatibility complex (MHC) class I (G); a positive signal with antibodies against CD11a/18 (A), CD105 (F) and MHC class II (H) partially overlapped with the negative control; no positive signal was detected with antibodies against CD34 (B) and CD45 (D). The dotted line represents the negative control. The horizontal line in individual histograms indicates the population of the positive cells.

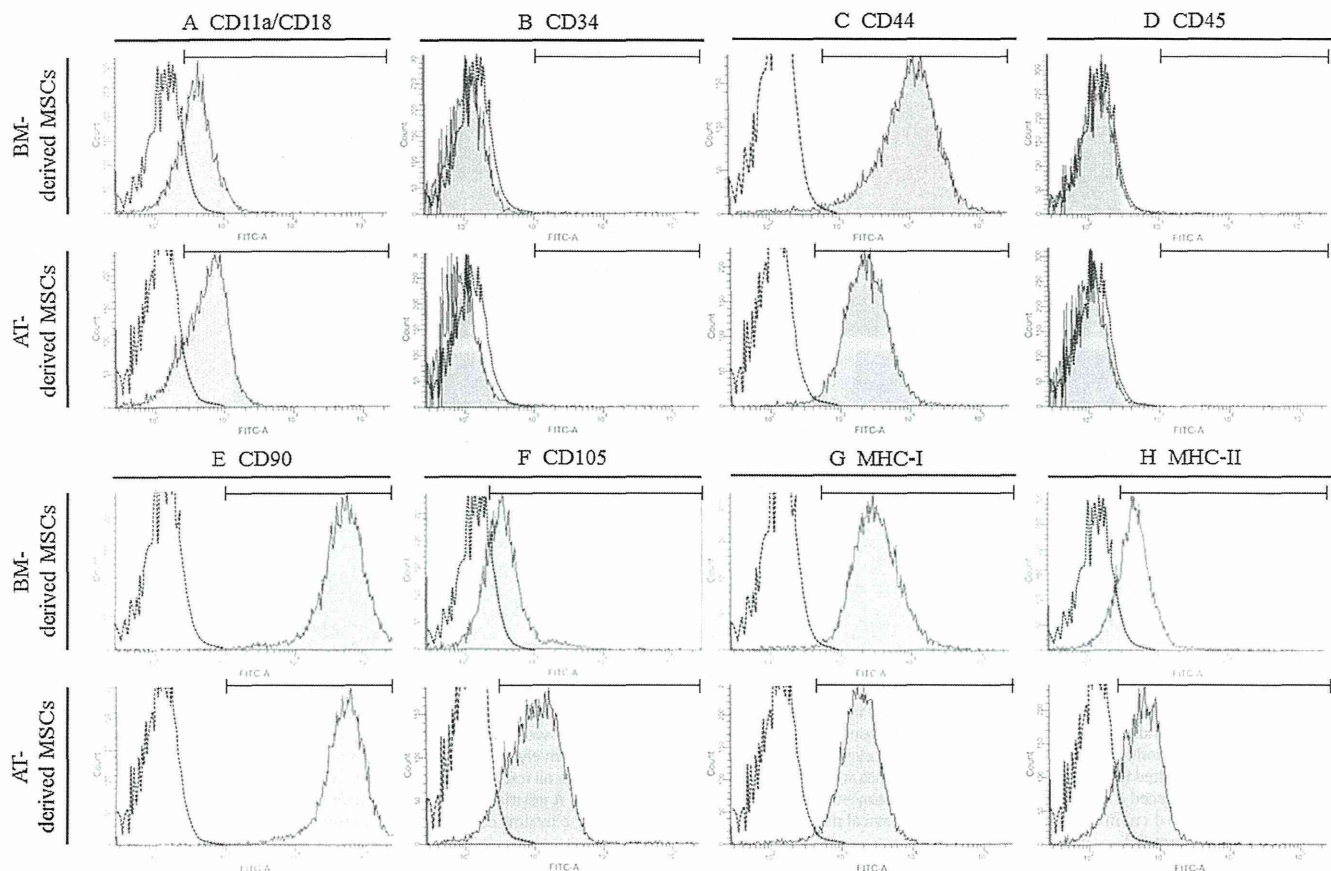


Fig. 4. Results of flow cytometry using the same markers as in Fig. 3 on adipose tissue (AT)-derived and bone marrow (BM)-derived mesenchymal stem cells (MSCs). A strong shift in mean fluorescence intensity (MFI) was detected with antibodies against CD44 (C), CD90 (E) and major histocompatibility complex (MHC) class I (G); a positive signal with antibodies against CD11a/18 (A), CD105 (F) and MHC class II (H) partially overlapped with the negative control; no positive signal was detected with antibodies against CD34 (B) or CD45 (D). The dotted line represents the negative control. The horizontal line in individual histograms indicates the population of the positive cells. The signal patterns were similar to those in synovial fluid (SF)-derived MSCs.

(62–364 colonies) was significantly ($P=0.001$) higher than the number from normal joints (0–21 colonies) (Table 2). SF-MSCs isolated from diseased joints proliferated to $>1 \times 10^6$ cells at P3 and 1×10^7 cells at P4 (Fig. 1a). Total cell doubling numbers were 1.81 ± 0.94 , 3.93 ± 1.11 and 5.83 ± 0.54 at P2, P3 and P4, respectively (Fig. 1b). Daily duplication rates were 0.20 ± 0.11 , 0.23 ± 0.12 and 0.25 ± 0.11 at P2, P3 and P4, respectively (see Appendix: Supplementary Fig. S1).

AT-MSCs and BM-MSCs could be transferred repeatedly to the next passage at intervals of 6 days, whereas the interval for SF-MSCs was 9 days. However, the doubling times of SF-MSCs were not significantly different from those of AT-MSCs and BM-derived MSCs (BM-MSCs) (see Appendix: Supplementary Fig. S2).

Reverse transcription-PCR and flow cytometry of stromal cells

Positive expression of Nanog and Sox2 in SF-MSCs was confirmed by RT-PCR (Fig. 2a). Expression of immunological markers on SF-MSCs is shown in Figs. 3 and 4, and Table 5. More than 90% of cells were positive for CD44, CD90 and MHC class I (Figs. 3c, e and g) and 60–80% of cells were positive for CD11a/18, CD105 and MHC class II, overlapping with the negative control (Figs. 3a, f and h), whereas no signal was detected with antibodies against CD34 and CD45 (Figs. 3b and d). Equine mononuclear blood cells were positive for CD34 and CD45 (see Appendix: Supplementary Fig. S3), as previously reported (Barberini et al., 2014; Mohanty et al., 2014).

No statistical difference in flow cytometry was observed between the SFs from the normal and diseased joints (P values for CD11a/18, CD34, CD44, CD45, CD90, CD105, MHC-I and MHC-II were 0.013, 0.714, 0.7, 0.768, 0.317, 0.372, 0.639 and 0.45, respectively). The results of SF-MSCs corresponded to those of AT-MSCs and BM-MSCs (Fig. 4).

Differentiation

After 2 weeks of osteogenic induction, SF-MSCs aggregated and contracted to form colonies, with expression of Runx2, ALP and OC (Fig. 2b). These cell clusters produced a specific matrix, including calcium apatite crystals, which stained positively with alizarin red (Fig. 5a, negative control is shown in Fig. 6a).

Adipogenic induction of MSCs resulted in adipocyte-like flattened cells with small lipid vesicles that stained positively with oil red O (Fig. 5b, negative control is shown in Fig. 6b). RT-PCR revealed the expression of the adipogenic marker gene PPAR- γ 2 (Fig. 2c).

The plate culture of SF-MSCs in chondrogenic induction medium induced a change in cell shape to a 'stone-wall' structure, followed by formation of a gelatinous monolayer that stained intensely with Alcian blue (Fig. 5c, negative control is shown in Fig. 6c). Blue sheets were also formed by chondrogenic induction of SF-MSCs at P10 (Fig. 7a) and SF-MSCs from normal joints (Fig. 7b). However, AT-MSCs and BM-MSCs formed no blue gelatinous sheets